Subm. Photonics. Tech. Lett. 5/7/95

1031

Investigation of fibre grating based performance limits in pulse stretching and recompression schemes using bidirectional reflection from a linearly chirped fibre grating.

D.Taverner, D.J. Richardson, M.N.Zervas, L.Reekie, L. Dong and J.L. Cruz

Optoelectronics Research Centre,
University of Southampton,
SO17 1BJ, UK.

Abstract:

We demonstrate the controlled stretching and recompression of ultrashort optical pulses using bidirectional reflection from both ends of a single linearly chirped fibre grating. We identify operating regimes for minimal pulse distortion due to the phase and filtering responses of a simple linear grating and experimentally demonstrate complete pulse reconstruction.

Investigation of the fibre grating based performance limits in pulse stretching and recompression schemes using bidirectional reflection from a linearly chirped fibre grating.

D.Taverner, D.J. Richardson, M.N.Zervas, L.Reekie, L. Dong and J.L. Cruz

Optoelectronics Research Centre,
University of Southampton,
UK.

The controllable dispersion characteristics of chirped fibre Bragg gratings offers many potential uses in all-fibre pulse shaping schemes. An example of this is fibre based chirped pulse amplification (CPA) [1,2] in which significant increases in pulse energies (~10μJ [1]) can be obtained for ps-fs pulses by stretching the pulses prior to, and then recompressing after, amplification within an erbium doped fibre amplifier (EDFA). This stretching circumvents limits imposed by disruptive nonlinear effects occurring at high pulse peak powers. The final pulse quality from such schemes is governed by the quality of the pulse stretching and compression process.

In the simplest form of fibre stretcher-compressor two fibre gratings of opposite chirp are employed. Chirping the gratings causes the effective reflection points of the incident wavelengths to be distributed along the grating length creating a highly dispersive reflection element to stretch the pulse. A similar grating of opposite dispersion can be used to recompress the pulse. The width of the pulse on leaving the first grating is determined by the length of the gratings used and the fraction of the grating bandwidth covered by the input pulse spectrum. Since the total relative time-delay for all wavelengths across the pulse bandwidth must be zero after the stretch-compress process close matching of the two grating reflection response characteristics is required to obtain suitable performance. Furthermore, the phase and amplitude responses of a simple linearly chirped grating exhibit a ripple which can not be easily compensated for, leading to an appreciable degradation in the output pulse quality [3]. In this letter we report on the performance limits of an alternative pulse stretcher-compressor based on the use of a single linearly chirped grating [4]. Pulses are stretched by reflection from one end of the grating and recompressed by reflection from the other. By using this bidirectional reflection approach the stretching and compression processes are automatically matched and the overall effect of the non-ideal grating response is reduced. Consequently, the results obtained using this scheme represent the limit as to the pulse quality that can be obtained from configurations based on simple linearly chirped gratings.

The performance of a single grating pulse stretcher-compressor was examined using the experimental set-up shown in Fig.1. Transform-limited pulses of tunable duration were launched into the circuit and the output pulse forms were compared with those at the input. The source was a mode-locked, 80m, polarisation switched, erbium-doped fibre (6m) ring laser capable of producing transform limited soliton pulses of T=2-11ps halfwidth at 1553nm. A single 2.1cm, 2.5 nm bandwidth ($\Delta\lambda_{grating}$), 98% reflectivity linearly chirped grating was used as both the pulse stretcher and compressor in a loop configuration with an amplifier providing sufficient gain to compensate the system losses. The linearly chirped grating was fabricated by writing a uniform grating into a stressed, tapered fibre using a phase mask technique [5,6]. The 200m dispersion shifted fibre (DSF) and modulator (40% on-off duty cycle, operated at the loop round trip) were included to prevent lasing within the loop. The losses accrued in the modulator and double pass through the 3dB coupler ensured pulse linearity within the DSF. The temporal and spectral forms of the input and output pulses were analyzed using an autocorrelator and optical spectrum analyzer.

Initially, we examined the stretching of the pulses due to a single reflection from one end of the grating as a function of the ratio of the pulse spectral 3dB bandwidth $\Delta\lambda_{pulse}$ (≈0.32/T) to the grating 3dB bandwidth ($\Delta\lambda_{pulse}/\Delta\lambda_{grating}$). In Fig.2 we show pulse-forms of the stretched pulses as measured on a fast diode and sampling scope with ≈17ps total resolution, for $\Delta\lambda_{pulse}/\Delta\lambda_{grating}$=0.14 and 0.63. In the case of the larger bandwidth ratio (Fig.2B) the pulse has broadened up to 159ps, an approximately eighty-fold increase in the pulse width. Fabry-Perot-type resonances within the grating are clearly manifest as multiple time domain peaks in the pulse; these resonances also appear as ripples in the spectral response of the grating. The 0.24nm separation of the most clearly observable peaks in the grating transmission spectrum was found to correlate well with the observed time domain peak separation which varied from 50-

15ps across the pulse. For the reduced bandwidth ratio case (Fig.2A) the pulse is only broadened to 51ps, but the flatter grating response over the pulse bandwidth results in less distortion to the stretched pulse.

We next investigated the quality of the overall pulse stretching-recompression. In Fig.3 we plot the observed temporal broadening of the output pulse (ratio of halfwidths of the Autocorrelation Functions (ACFs)) as a function of $\Delta\lambda_{pulse}/\Delta\lambda_{grating}$. The plot shows that the disruptive effects of the non-ideal grating response observed in Fig.2 become noticeable for $\Delta\lambda_{pulse}/\Delta\lambda_{grating}>0.2$. In Fig.4 we show the input and output ACFs for the case $\Delta\lambda_{pulse}/\Delta\lambda_{grating}=0.1$. The ACFs are identical indicating almost perfect stretching and recompression of the pulses. Outside this limit incomplete recompression of the pulses is obtained resulting in pulse broadening and the development of pedestal components (see Fig.5). Since the grating spectral response was almost flat-topped and the bandwidth greater than that of the input pulses the observed spectral shaping was very small (the FWHM (full width at half maximum) being narrowed by less than 4% in the worst case), only becoming noticeable for the larger input bandwidths as a cut-off in the wings of the pulse. The system was modelled numerically using a fit of the transmission intensity response of a linearly chirped Bragg reflector, calculated with coupled mode theory, to the transmission spectra of the grating. The dotted curve in fig.3 represents data obtained from reflected pulse ACF widths using the model, showing a very close fit to the experimental data. Once validated, the model was applied to a range of linearly chirped gratings of various lengths and strengths, showing similar limits concerning the loss of pulse quality.

In conclusion, we have identified a regime of high quality chirp control for reflection of optical pulses from this linearly chirped fibre grating given roughly by $\Delta\lambda_{pulse}/\Delta\lambda_{grating} \leq 0.2$. Beyond this limit we have directly observed the distortive effects of its non-ideal phase and amplitude response. These experiments give us clear design criteria for selecting fibre gratings for use in applications such as CPA where the overall pulse quality is a key issue. In this regime system performance becomes a trade-off between the limits imposed by the grating distortion of the pulse and the benefits of utilising a greater proportion of the grating bandwidth. Apodisation of the grating edges has been proposed as a technique to improve the phase response of such gratings [3]; however, it should be remembered that, for a fixed length, apodisation of a chirped grating results in a reduced grating bandwidth which can itself lead to additional pulse broadening.

References:

[1] A. Galvanauskas, M. E. Fermann, P. Blixt, J. A. Tellefsen, D. Harter: "Hybrid diode-laser fiber-amplifier source of high energy short pulses", Opt. Lett., 19, pp1043-1045, (1995).

[2] A. Galvanauskas, M. E. Fermann, D. Harter, K. Sugden, I. Bennion: "All-fiber femtosecond pulse amplification circuit using chirped Bragg gratings", Appl. Phys. Lett., 66, pp.1053-1055 (1995).

[3] K. O. Hill, F. Bilodeau, B. Malo, T. Kitagawa, S. Theriault, D.C. Johnson, J. Albert and K. Takiguchi: "Chirped in-fiber Bragg gratings for compensation of optical fiber dispersion", Opt. Lett., 19, pp1314-1316, (1994).

[4] A. Boskovic, J. R. Taylor, R. Kashyap: "Dispersive broadening and complete recompression of femtosecond pulses in a chirped Bragg fiber grating", Tech. Digest CLEO '95, 15, CMG4, pp.30-31, (1995)

[5] M. A. Putnam, G. M. Williams, and E. J. Friebele: "Fabrication of tapered, strain-gradient chirped fibre Bragg gratings", Elec. Lett., 31, pp.309-310, (1995).

[6] L. Dong, J. L. Cruz, L. Reekie and J. A. Tucknott: "Fabrication of chirped gratings using etched tapers", Elec. Lett.,31, pp.908-909, (1995).

Captions:

Figure 1: Experimental setup. The inset shows the transmission spectrum of the grating used.

Figure 2: Directly detected intensity profile of pulses broadened by a single reflection from the linearly chirped grating for $\Delta\lambda_{pulse}/\Delta\lambda_{grating}$ = 0.14 and 0.63 in A and B respectively. The input spectra are shown inset.

Figure 3: The temporal broadening factor of the stretched and recompressed pulses for a variety of input pulses. The dotted curve represents output from a theoretical model of the system.

Figure 4: Input and output pulse autocorrelation traces after stretching and recompression for $\Delta\lambda_{pulse}/\Delta\lambda_{grating}$ = 0.1. The pedestal level was produced by the source laser when operated at the extreme of it's pulse duration range. The input spectrum is shown inset.

Figure 5: Input (dotted line) and output (solid line) pulse autocorrelation traces after stretching and recompression for $\Delta\lambda_{pulse}/\Delta\lambda_{grating}$ = 0.5.

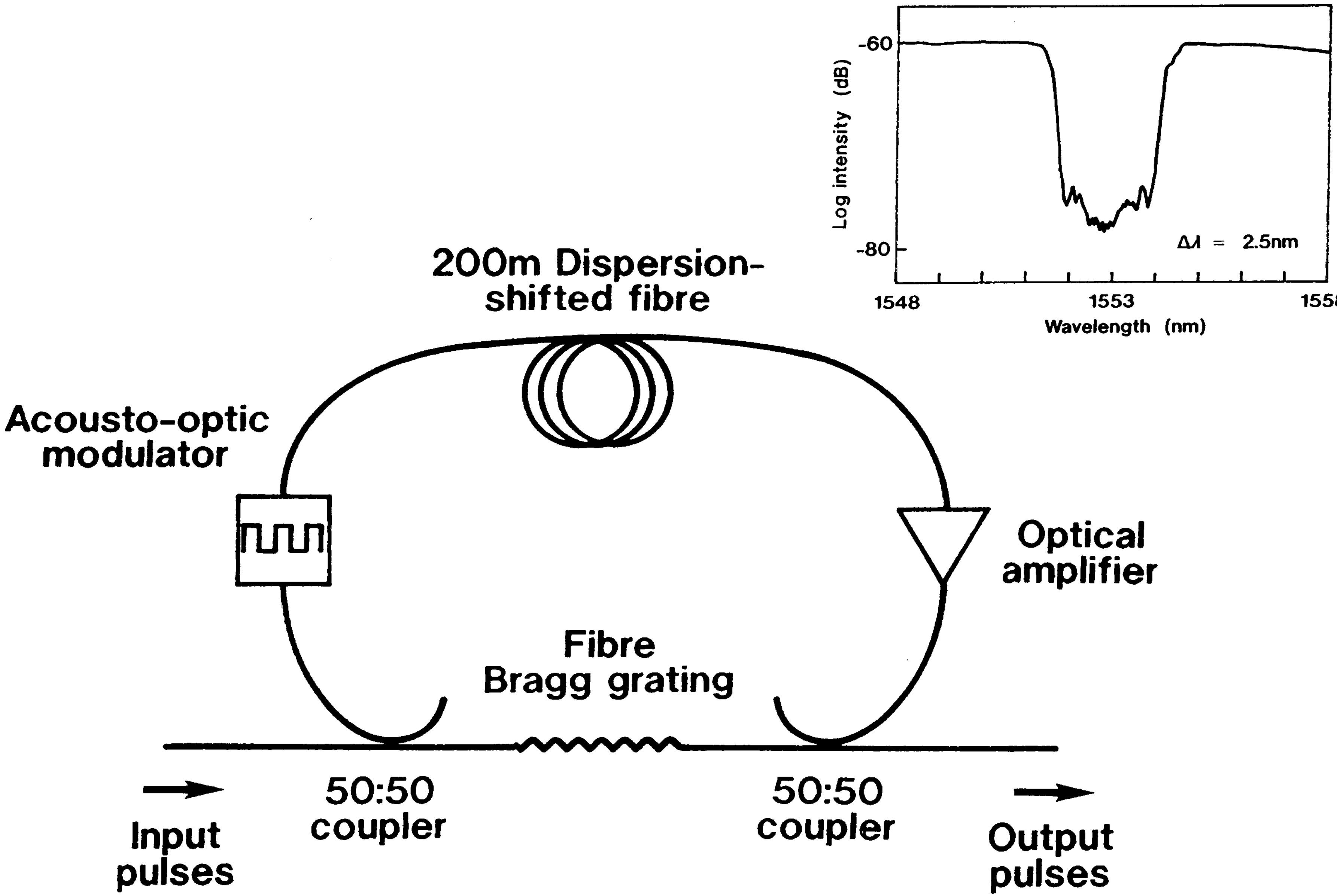

-60
-80
Log intensity (dB)
Δλ = 2.5nm
1548
1553
1558
Wavelength (nm)
200m Dispersion-
shifted fibre
Acousto-optic
modulator
Optical
amplifier
Fibre
Bragg grating
50:50
coupler
50:50
coupler
Input
pulses
Output
pulses

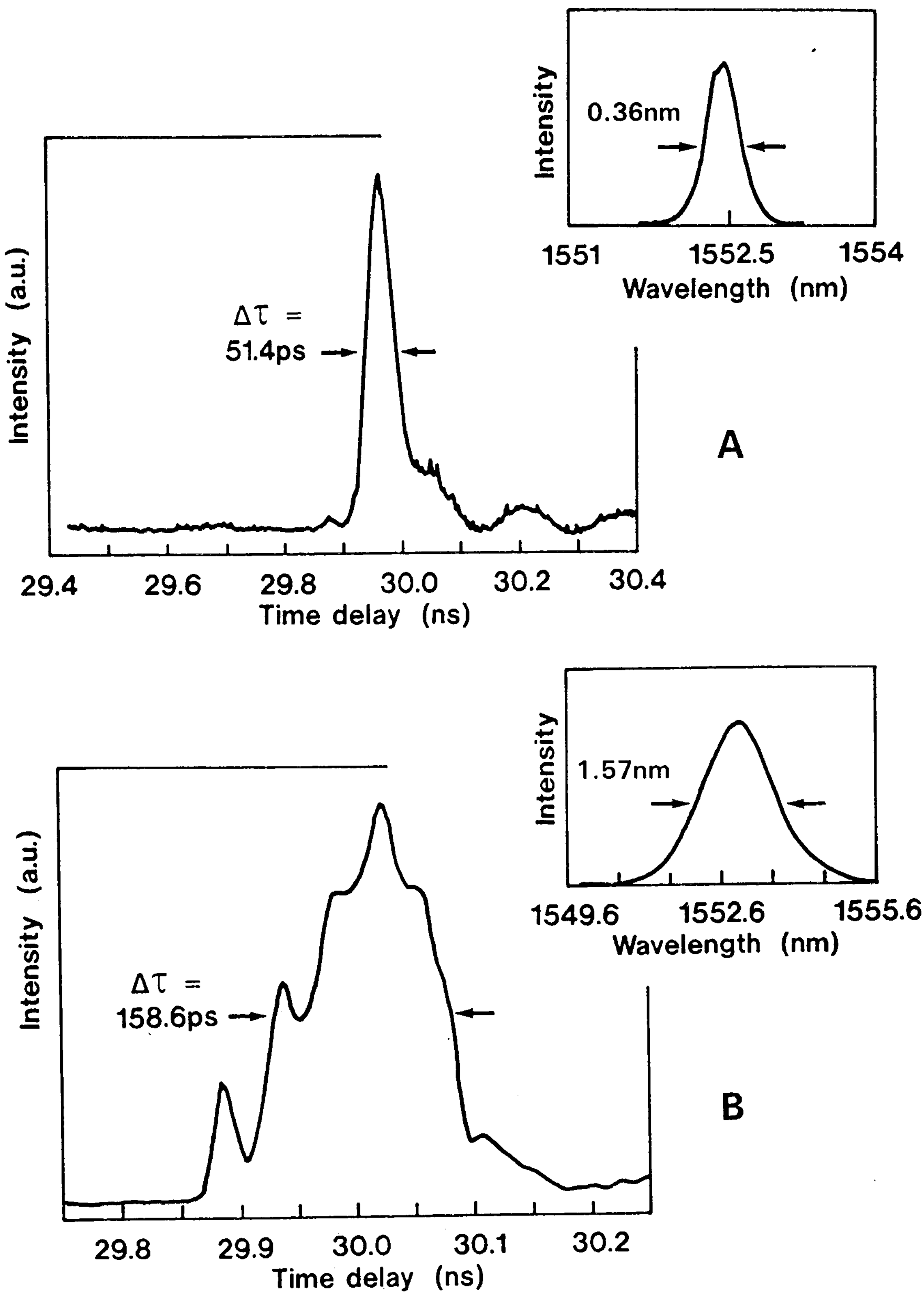
Intensity
0.36nm
1551
1552.5
1554
Wavelength (nm)
Intensity (a.u.)
Δτ =
51.4ps
A
29.4
29.6
29.8
30.0
30.2
30.4
Time delay (ns)
Intensity
1.57nm
1549.6
1552.6
1555.6
Wavelength (nm)
Intensity (a.u.)
Δτ =
158.6ps
B
29.8
29.9
30.0
30.1
30.2
Time delay (ns)

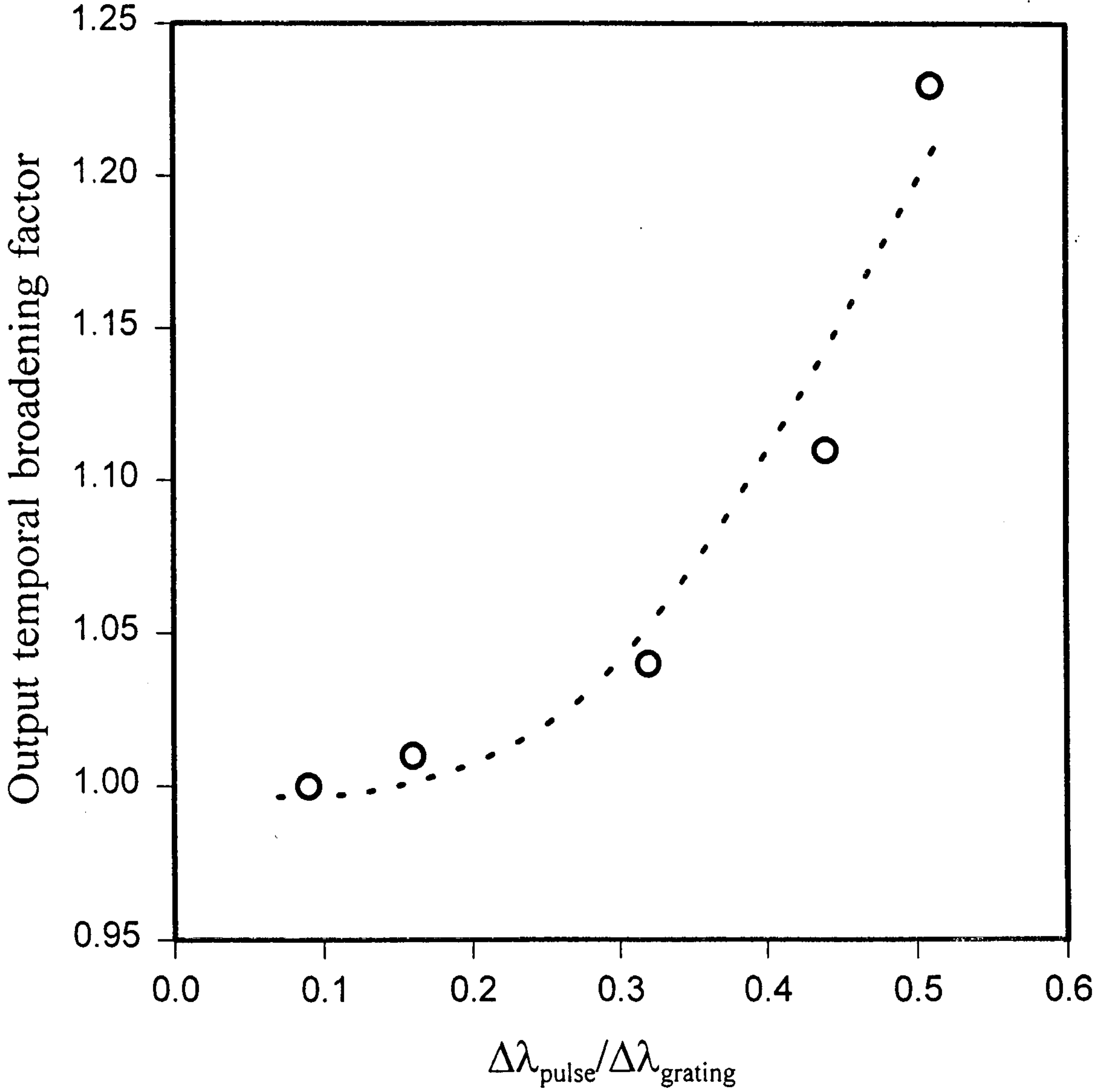

Output temporal broadening factor
1.25
1.20
1.15
1.10
1.05
1.00
0.95
0.0
0.1
0.2
0.3
0.4
0.5
0.6
$\Delta\lambda_{pulse}/\Delta\lambda_{grating}$

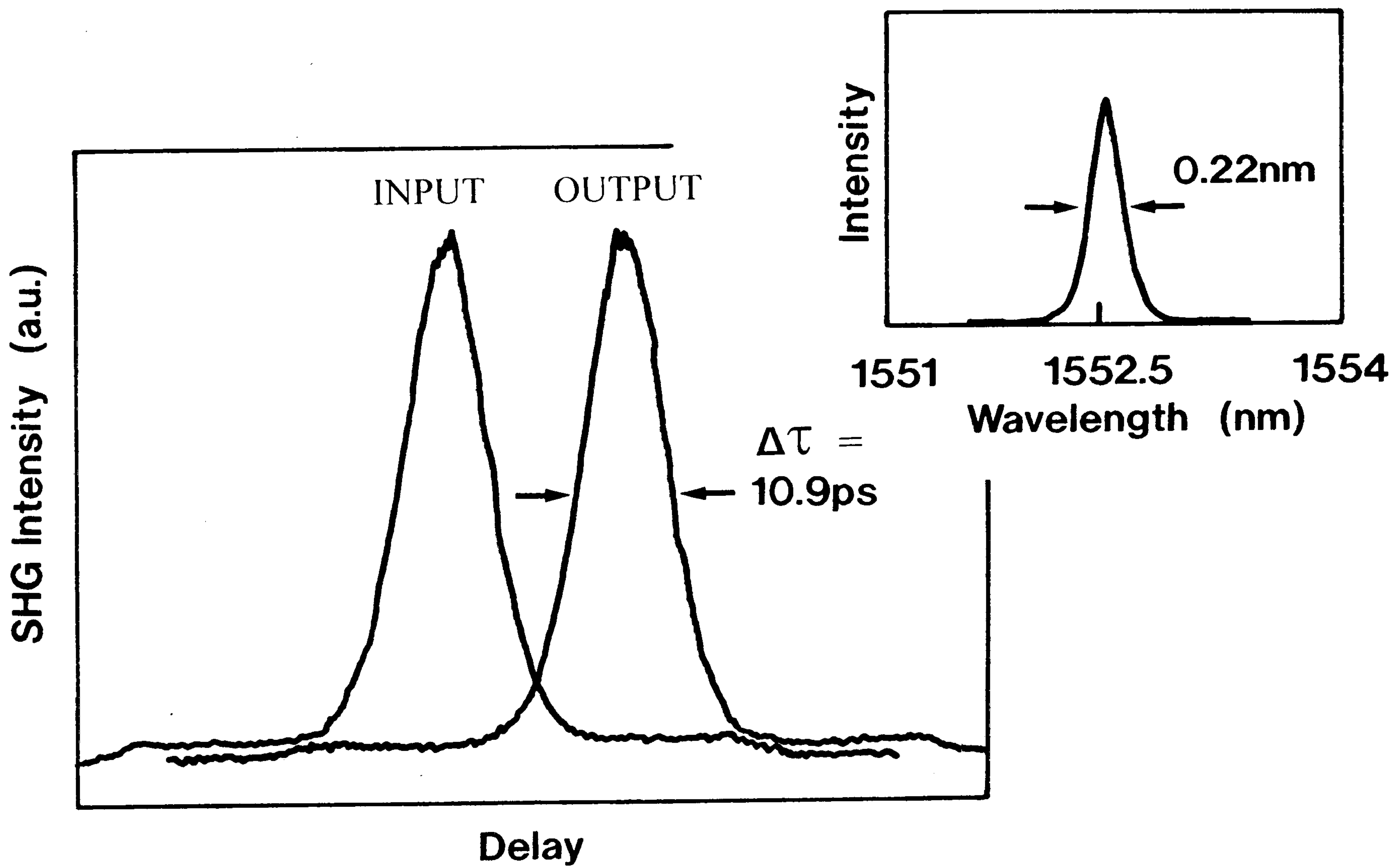

INPUT
OUTPUT
SHG Intensity (a.u.)
Delay
Δτ = 10.9ps
Intensity
0.22nm
1551
1552.5
1554
Wavelength (nm)

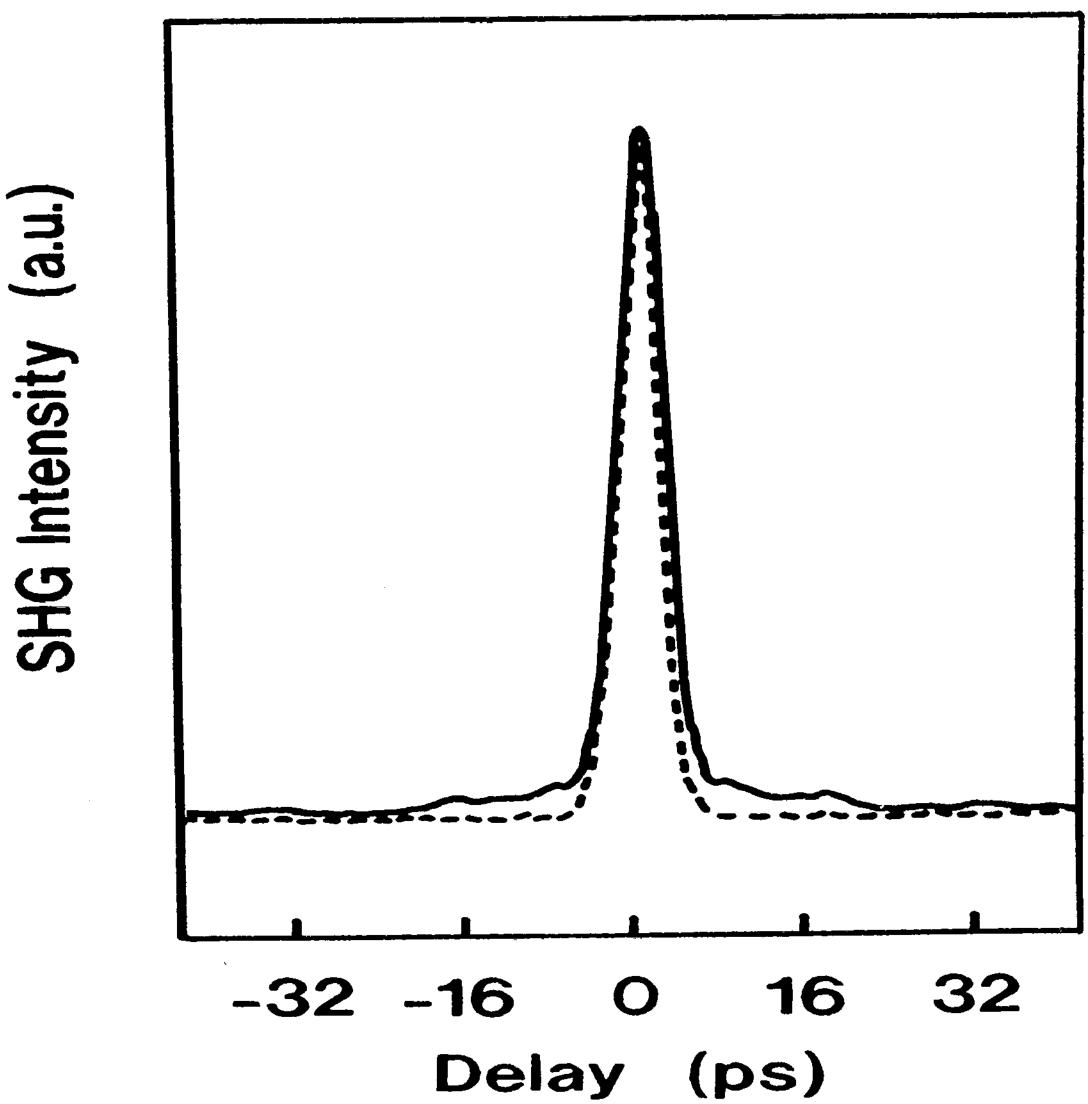
SHG Intensity (a.u.)
-32
-16
0
16
32
Delay (ps)